Food Chemistry: X 20 (2023) 101038

Contents lists available at ScienceDirect

Food Chemistry: X

journal homepage: www.sciencedirect.com/journal/food-chemistry-x

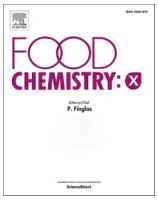

Proteomic and metabolomic analysis of ageing beef exudate to determine that iron metabolism enhances muscle protein and lipid oxidation

Jun Liu [a,b,d], Cuili Pan [c,d,*], Hui Yue [a], He Li [a], Dunhua Liu [d], Ziying Hu [d], Yuanliang Hu [a,b], Xiang Yu [a,b], Weiwei Dong [a], Yanli Feng [a]

[a] Hubei Key Laboratory of Edible Wild Plants Conservation & Utilization, College of Life Sciences, Hubei Normal University, Huangshi 435002, China
[b] Hubei Engineering Research Center of Special Wild Vegetables Breeding and Comprehensive Utilization Technology, Hubei Normal University, Huangshi 435002, China
[c] Key Laboratory of Animal Genetics, Breeding and Reproduction of Shaanxi Province, College of Animal Science and Technology, Northwest A&F University, Yangling 712100, China
[d] Faculty of Life and Food Sciences, Ningxia University, 750021 Yinchuan, China

ARTICLE INFO

Keywords:
Exudate
Beef
Ageing
Oxidation
Iron metabolism

ABSTRACT

The study aimed to assess differences in proteomic and metabolite profiles in ageing (1, 2, 4, and 6 days at 4 °C) beef exudates and determine their relationship with beef muscle iron metabolism and oxidation. Proteomic and metabolomic analyses identified 877 metabolites and 1957 proteins. The joint analysis identified 24 differential metabolites (DMs) and 56 differentially expressed proteins (DEPs) involved in 15 shared pathways. Ferroptosis was identified as the only iron metabolic pathway, and 4 DMs (L-glutamic acid, arachidonic acid, glutathione and gamma-glutamylcysteine) and 5 DEPs (ferritin, phospholipid hydroperoxide glutathione peroxidase, heme oxygenase 1, major prion protein, and acyl-CoA synthetase long chain family member 4) were involved in iron metabolism by regulating heme and ferritin degradation, Fe^{2+} and Fe^{3+} conversion, arachidonic acid oxidation and inactivation of glutathione peroxidase (GPX) 4, leading to increased levels of free iron, ROS, protein and lipid oxidation ($P < 0.05$). Overall, abnormal iron metabolism during ageing induced oxidative stress in muscle tissue.

1. Introduction

Postmortem ageing is a common treatment in the meat industry and is a value-adding process for the muscle (Kim et al., 2018). In the process of muscle conversion into meat, there are intrinsic biophysical/biochemical changes, which subsequently have a direct impact on the quality attributes of the meat. Muscle mass is a combination of many factors, including meat taste, color, storage stability and nutrition (Yu et al., 2023). For example, the degradation of cytoskeletal myofibrillar protein by endogenous proteases during the ageing process has been shown to enhance the tenderization of meat. Concurrently, the liberation of flavor-related compounds, including nucleotide moieties, carbohydrates participating in the Maillard reaction, aldehydes, and ketones, as well as other lipid oxidation products, contributes to an enhancement in gustatory appeal (Kim et al., 2018; Lepper-Blilie, Berg, Buchanan & Berg, 2016). Overall, ageing had a significant positive effect on the sensory qualities of meats. Nevertheless, protracted ageing is prone to exert negative impact on the color, protein and lipid oxidative stability of meat, as well as expedite the eventual onset of meat discoloration and oxidation-driven olfactory anomalies (Yu, Cooper, Sobreira & Kim, 2021; Yu et al., 2023). Besides, the oxidation of protein can induce the forfeiture of tertiary structure and expose folded hydrophobic amino acid residues, thereby detrimentally influencing the water-binding capacity of protein (Liu, Liu, Zheng & Ma, 2022). Thus, obtaining a comprehensive understanding of the early biochemical changes in postmortem is imperative in order to assess the inherent driving forces underpinning muscular quality.

Fresh meat is typically stored in sealed or vacuum packages, and this wet-ageing treatment is the most frequently applied ageing method (Kim et al., 2018). During the wet ageing process, substances, such as proteins and inorganic salts, dissolve in the water of the tissue medium, and are inevitably released into the package as exudate upon muscle segmentation (Setyabrata et al., 2023). Consequently, the exudate contains a plethora of biochemical components, such as lactic acid, ATP, short-chain fatty acids, amino acids, tyrosine and myoglobin, among others, that could potentially serve as substrates for analysis (Liu, Hu, Zheng,

* Corresponding authors at: Northwest A&F University, 22 Xinong Road, Shaanxi, 712100, Yangling, China (C. Pan).
E-mail addresses: jliu@hbnu.edu.cn (J. Liu), 13466552406@163.com (C. Pan), ldh320@nxu.edu.cn (D. Liu).

https://doi.org/10.1016/j.fochx.2023.101038
Received 15 August 2023; Received in revised form 12 November 2023; Accepted 25 November 2023
Available online 30 November 2023

Ma & Liu, 2022). It should be noted that muscle exudate is not constant, but rather, the result of a cascade of biochemical reactions, encompassing glycogenolysis, glycolysis, oxidative phosphorylation, fatty acid metabolism, and iron metabolism, among other processes. The exudate has been reported to provide a valuable source of information, which correlates with meat quality features, including color, tenderness and water-holding capacity (Liu, Hu, Liu, Zheng & Ma, 2023; Setyabrata et al., 2023; Yu et al., 2023). It is important to emphasize that the analysis of muscle mass requires the cutting of muscle tissue, which is a destructive method (Zhang, Yu, Han, Han & Han, 2020). Exudate, on the other hand, is a non-destructive experimental sample of fluid that is released into the environment (Setyabrata et al., 2023). Overall, as an easily accessible analytical matrix, it can be used to probe the mechanisms underlying changes in muscle quality.

The changing patterns of muscle quality during aging have been reported, for example, the effect of age on muscle metabolites, the relationship between apoptosis and tenderness and the effect of pH on meat color (Chen et al., 2020; Marcondes Krauskopf et al., 2023; Wang, Li, Zhang, Li, Yang & Wang, 2023). These studies have not addressed the mechanisms by which specific metabolic pathways occur, particularly the effect of iron on muscle metabolism and quality. This is because beef is considered red meat and contains higher levels of iron ions (Liu, Liu, Zheng & Ma, 2022). Iron metabolism is an essential intracellular metabolic process, as iron is a vital component of numerous proteins and enzymes within the biological organisms, participating in a multitude of physiological processes, such as oxygen transport, energy metabolism and immune function (Liu, Liu, Wu, Pan, Wang & Ma, 2022). On the other hand, disturbances in iron metabolism may result in the overproduction of free radical substances, provoking oxidative stress within cells (Wang et al., 2023). Nevertheless, the iron metabolism process is a sophisticated biological system, and it is necessary to use effective techniques to elucidate the variation in muscle quality throughout the ageing process by exploring the metabolic pathways. Utilizing metabolomics analysis of exudate, we have identified reductions in muscle quality resulting from anomalies in iron metabolism during the ageing process (Hu et al., 2022; Liu et al., 2023). Proteomics and metabolomics techniques have achieved ubiquitous application in the quest for biological markers of meat quality traits, concurrently allowing for the characterization of the interplay between a multitude of biological functions, including protein and metabolite chemistry, signal transduction pathways and gene expression patterns (Huang et al., 2023). Thus, these techniques provide a comprehensive account of the mechanisms responsible for alterations in the components and biological processes relevant to meat quality.

Considering the intricate nature of iron metabolism and meat quality change characteristics, the exudate samples from bovine muscles aged 1, 2, 4 and 6 days were collected, and examined through proteomics and metabolomics analyses, revealing a comprehensive picture of the proteins and metabolites present in the exudate mixtures. A combination of proteomics with bioinformatics was used to analyze muscle iron metabolism pathways during ageing and explore the intrinsic mechanisms affecting muscle quality. This study evaluates the potential application of exudate for probing the substrates of muscle quality changes and provides new insights into the patterns of muscle quality changes during aging. The study may provide fundamental data for meat quality analysis, prediction and development of characterization marker systems.

2. Materials and methods

2.1. Sample collection

The muscle samples were aged and exudates (EXU) were collected according to our previous report (Liu et al., 2023). In brief, eight adult Qinchuan cattle (bulls, 18–24 months of age, weighing approximately 400 kg) were slaughtered at a commercial slaughterhouse (Yitai Co., Yongning, China) according to Chinese livestock slaughter protocols. Muscle samples (*M. longissimus lumborum* muscles) were collected after slaughter, and were divided into cubes with sides of 2.5 cm thickness and 100.0 ± 2.5 g weight, placed on PET plastic trays and wrapped in polyvinyl chloride cling film. The muscle samples were divided into 4 groups of 6 pieces each and aged at 4 °C for 6 days (Foshan City Aslok Refrigeration Equipment Co., Ltd., Foshan, China). EXU were aspirated on days 1, 2, 4 and 6, named as EXU1, EXU2, EXU4 and EXU6, respectively. Samples were taken at the center of the muscle tissue for freezing in liquid nitrogen and then stored in a −80 °C cryopreservation chamber (Qingdao Haier Biomedical Co., Qingdao, China) for proteomic, metabolomic, physiological and biochemical analyses.

2.2. Determination of iron ion content in exudate and beef

The collected exudate samples were thawed at 2–4 °C and centrifuged at 3000 × *g*, 4 °C for 15 min. The supernatant was removed and the iron content in EXU was determined using a fully automated biochemical analyzer (Chemray 240, Radu Life, Shenzhen, China) according to the instructions of the iron assay kit (Huili Biotechnology Co., Ltd., Changchun, China).

The 30 g of muscle were minced, and 10.00 ± 0.02 g of minced meat were added into 100 mL of deionized water, then homogenized for 60 s and centrifuged at 12,000 × *g* for 10 min. The supernatant was separated through an Amicon Ultra-15 ultrafiltration centrifuge filter (3,000 MW cut-off) (Millipore, Massachusetts, USA), centrifuged at 4,500 × *g* for 50 min, and the liquid was collected at the bottom of the centrifuge tube. Then 4 mL of the filtrate was pipetted, and the free iron content was measured by ICP-OES (Agilent, Santa Clara, CA, USA).

2.3. Antioxidant status of exudate and beef

The EXU was thawed in an ice-water bath, centrifuged at 3500 × *g*, 4 °C for 10 min, and the supernatant was used for antioxidant analysis. The absorbance values were measured at 450 nm and 412 nm (UV-9000S Metash Instruments co, Ltd, Shanghai, China) to calculate the total superoxide dismutase (*T*-SOD) and glutathione peroxidase (GSH-PX) activities, respectively, referring to the kit manufacturer's instructions (Jiancheng BI, Nanjing, China). Carbonyl, sulfhydryl and malondialdehyde (MDA) levels were determined according to Liu et al. (2022) utilizing the manufacturer's instructions of a commercial kit (Jiancheng BI, Nanjing, China).

2.4. Muscle tissue reactive oxygen species (ROS) levels

ROS levels in muscle tissue were measured by the 2,7-dichlorofluorescein diacetate (DCFH-DA) method according to Zhang, Yu, Han, Han & Han (2020). Briefly, 5.00 ± 0.05 g of pulverized muscle samples were mixed with 20 mL of prechilled potassium phosphate buffer (10 mM Tris, 10 mM sucrose, 0.8 % NaCl, 0.1 mM EDTA-2Na, pH 7.4), and then homogenized for 60 s and centrifuged at 10,000 × *g*, 4 °C for 20 min. Then, 5 mL supernatant was mixed with 5 mL potassium phosphate buffer (containing 10 μM DCFH-DA) and incubated at 37 °C in the dark for 35 min. A fluorescence spectrophotometer (Yidian Scientific Instruments Co., Shanghai, China) with an excitation wavelength of 480 nm and an emission wavelength of 525 nm was used to measure fluorescence intensity before and after incubation. The ROS level was expressed as the ratio of fluorescence intensity before and after incubation to protein concentration and incubation time.

2.5. Proteomics analysis

The EXU samples were thawed in an ice water bath after removal from the −80 °C refrigerator. Exudates were thawed only once to avoid repeated freeze-thawing. Then 100 μL of exudate were added to 400 μL of SDT lysate buffer (4 % sodium dodecyl sulfate, 100 mM Dithiothreitol, 150 mM Tris-HCl, pH 8.0) and the mixture was sonicated in an

ice bath for 2 min. Undissolved impurities were removed using centrifugation at 16,000 × *g* for 15 min, and the supernatant was collected, and the concentration of exudate proteins was quantified according to the instructions of the BCA Protein Assay Kit (Bio-Rad, CA, USA).

Protein digestion, TMT peptide labelling, peptide classification and LC-MS/MS analysis were performed referring to our previous report (Liu et al., 2022). In a nutshell, protein extracts from muscle samples were subjected to trypsin (Promega Co.) digestion and purified peptides were collected. The extracted peptides were labelled using TMT labelling kits according to the manufacturer's instructions (Thermo Fisher, MA, USA), and the dried peptides were fractionated using a high pH reversed-phase column (Pierce™ High pH Reversed-Phase Peptide Fractionation Kit, Thermo Fisher, MA, USA). The solubilized peptides were chromatographed (LC-MS) using a nanolitre flow rate chromatography system (Thermo Fisher, MA, USA). The peptides were separated and analyzed by DDA (data dependent acquisition) mass spectrometry using a mass spectrometer (Thermo Fisher, MA, USA).

The resulting LC-MS/MS raw RAW files were imported into the search engine Sequest HT in Proteome Discoverer software (version 2.4, Thermo Scientific) for database searching. The database used for the library search was uniprot-Bos taurus (Bovine) [9913]-47135–20220613.fasta from the URL https://www.uniprot.org/taxonomy/9913 protein database with protein entry: 47135; download date. 2022.06.13. The main library search parameters were set as shown below.

2.6. Metabolomics analysis

The untargeted metabolomic analysis of the exudate was performed according to our previous report (Liu et al., 2022). Untargeted metabolomics profiling was analyzed with a UPLC-ESI-Q-Orbitrap-MS system (Ultra High Performance Liquid Chromatography, Nexera X2 LC-30AD, Shimadzu CO., Kyoto, Japan; Q Exactive Plus combined quadrupole Orbitrap mass spectrometer, Thermo Scientific, CA, USA). Samples consisted of muscle exudate aged for 1, 2, 4 and 6 days and four sets of quality control (QC) samples with an equal volume mix of exudate. Metabolites were extracted from the exudate residue by vortexing 100 μL of a sample with 400 μL of 4 °C methanol–acetonitrile (*v/v*, 1:1) and sonicated in an ice bath for 1 h. The mixture was incubated at −20 °C for 1 h and then centrifuged at 14,000 × *g*, 4 °C for 20 min. The supernatant was collected and freeze-dried under a vacuum. The metabolites were separated using hydrophilic interaction liquid chromatography (HILIC) after re-dissolution using 50 % acetonitrile and filtration through 0.22 μm cellulose acetate. Mass spectrometric detection was performed using electrospray ionization (ESI) in positive and negative modes to acquire metabolite MS data.

2.7. Statistical analysis

P-values for proteins and metabolites were calculated using one-way analysis of variance (ANOVA) for multiple analyses with R 4.0.1 (The University of Auckland, New Zealand). Metabolites with variable influence on projection (VIP) values > 1.0 and *P*-value < 0.05 were considered to be statistically significant. Proteins with fold change (FC) ≥ 1.2 or ≤ 0.83 and $P < 0.05$ were considered to be statistically significant proteins. The main components of the combined metabolomics and proteomics analysis project flow using R 4.0.1 and Cytoscape 3.8.2 include network analysis, metabolite and protease correspondence table, combined metabolism-protein analysis KEGG metabolic pathway enrichment, and Total KEGG pathway analysis. All physicochemical experiments were performed in three parallel experiments. Data were tallied in Microsoft Excel using one-way analysis of variance (ANOVA) in SPSS 25 (IBM, NY, USA), followed by Tukey's analysis to calculate statistical differences between samples, with *P*-values < 0.05 considered statistically different.

3. Results

3.1. Exudate and beef oxidation status

As shown in Fig. 1, the iron ion levels in EXU did not differ significantly from 1 to 4 d and increased significantly ($P < 0.05$) at 6 d with a growth rate of 148.37 % compared to 1 d. Free iron levels in beef tissues significantly increased ($P < 0.05$) from 1 to 6 d. The increase in iron ion levels was accompanied by a significant decrease in *T*-SOD and GSH-PX activity in the exudate ($P < 0.05$). In contrast, beef tissue ROS levels increased significantly ($P < 0.05$) from 1 to 6 d, with a growth rate of 176.38 % compared to 1 d. Using carbonyl and sulfhydryl groups and malondialdehyde (MDA) to characterize the protein and lipid oxidation status of exudate and beef, exudate and beef exhibited the same status, with increased protein carbonyl and MDA levels and decreased sulfhydryl levels at 1–6 d, indicating enhanced protein and lipid oxidation. Notably, the increase in total protein levels in the exudate indicates the presence of macromolecules available for proteomics analysis.

3.2. Metabolomics profiling

Using a non-targeted metabolomics assay, 572 and 305 metabolites were identified from beef exudate in positive and negative ion mode (POS and NEG), respectively. To obtain a comprehensive overview of metabolite profiles and trends to assess whether metabolites could be used for differential metabolites (DMs) screening and bioinformatics analysis, principal component (PCA) and partial least squares (PLS-DA) analyses were performed in the identified metabolites. As shown in Fig. 2 a and d, PCA analysis showed no separation of quality control samples (QC) in POS and NEG, indicating reliable results for metabolite detection based on the LC-MS/MS system. PCA analysis showed a better overall separation compared to EXU1, but with some overlap. As shown in Fig. 2 b and e, pairwise comparison of the PLS-DA model for EXU1 and EXU2&4&6 metabolites revealed a good degree of separation between EXU1 and EXU2&4&6, indicating that the models reasonable and the identified metabolites can be used for the next step of analysis.

As shown in Fig. 2 c and f, a total of 278 DMs were identified in the POS and NEG using *t*-test (*P*-value ≤ 0.05) and variable influence on projection (VIP) ≥ 1 as screening criteria (**Table S1**). Cluster analysis of the identified DMs was performed (Fig. 2g), where the color change in the same column showed the pattern of metabolite variation (upregulation-orange, downregulation-blue). In addition, the DM superclasses were classified using KEGG, and the DMs were mainly organic acids and derivatives (39), organoheterocyclic compounds (32), lipids and lipid-like molecules (21), phenylpropanoids and polyketides (15), nucleosides, nucleotides and analogues (14), benzenoids (13), and organic oxygen compounds (12).

3.3. Proteomics profiling

The protein composition of the four groups of exudate samples was examined by TMT proteomics. Fig. 3a shows the expression patterns of the proteins in different groups with correlation coefficients (Corr) $>$ 0.995, indicating the reliable results based on the LC-MS system. A total of 1957 proteins were identified by annotation of protein peptides. The differentially expressed proteins (DEPs) were screened with a fold changes (FC) of > 1.2 fold (up > 1.2, down < 0.86) and a *t*-test *P*-value < 0.05 as the criteria (Fig. 3 b-d). A total of 295 DEPs were identified (**Table S2**). The clustering heat map analysis of DEPs is shown in Fig. 3e. The similar color of the same group of proteins indicates that the corresponding proteins have the same expression pattern, showing good intra-group similarity and inter-group variability. Secondly, the clustering heat map showed the changes of protein expression, with orange color indicating up-regulated protein expression and blue color indicating down-regulated protein expression (Fig. 3e). Overall, the proteomic identification of proteins in exudate showed reliable results, and

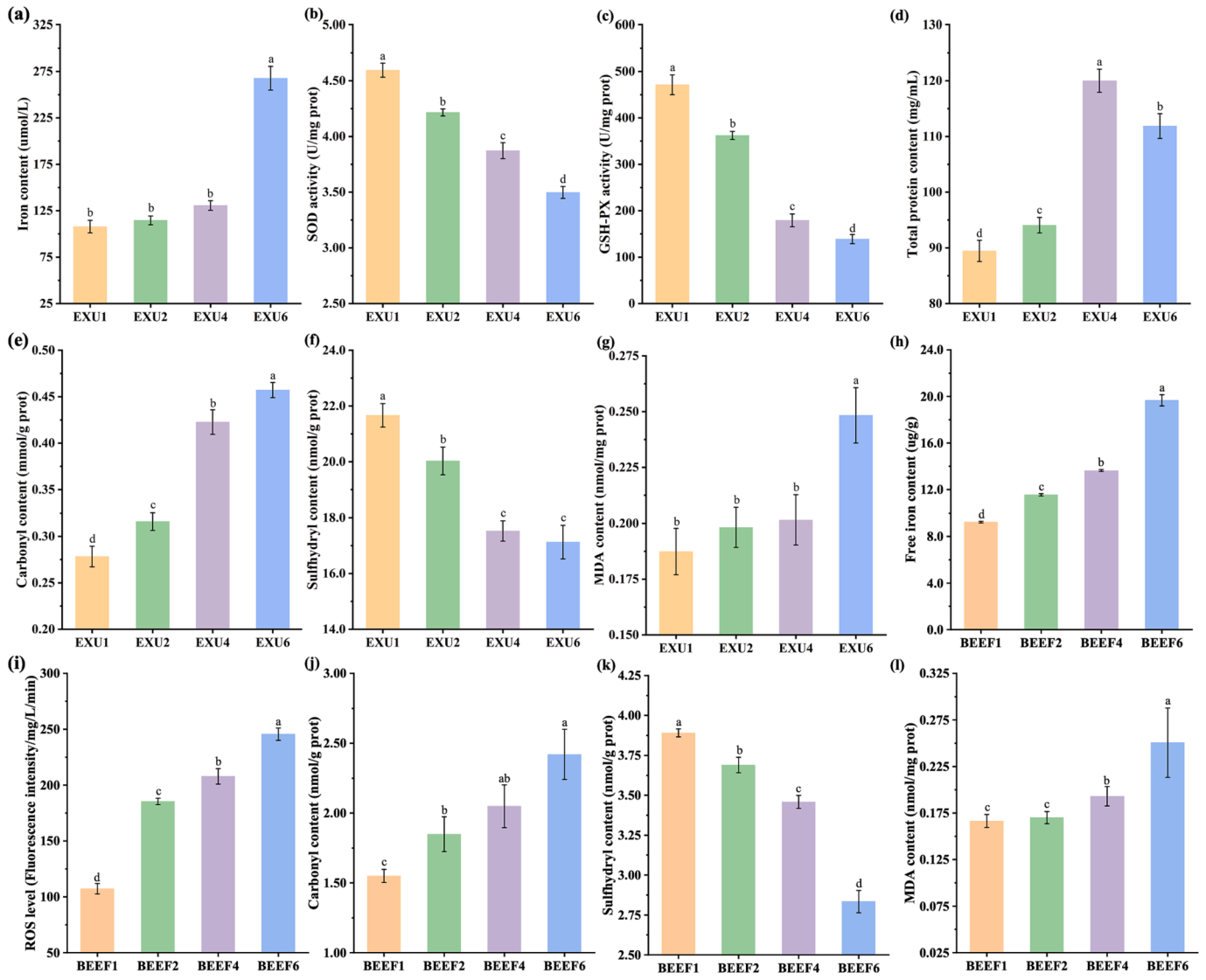

Fig. 1. Exudate and beef iron ion levels and oxidation status. (a) Iron content in exudate. (b) SOD activity in exudate. (c) GSH-PX activity in exudate. (d) Total protein content in exudate. (e) Protein carbonyl level in exudate. (f) Protein sulfhydryl level in exudate. (g) MDA level in exudate. (h) Free iron content in beef tissues. (i) ROS levels in beef tissues. (j) Protein carbonyl levels in beef tissue. (k) Protein sulfhydryl level in beef tissue. (l) Beef tissue MDA levels. a-e different lowercase letters indicate one-way *t*-test $P < 0.05$.

relevant DEPs were identified for subsequent bioinformatics analysis.

3.4. Analysis of the KEGG enrichment pathway

Fig. 4 a and b show the KEGG pathways that DMs and DEPs are enriched to, involving mainly cellular processes, environmental information processing, human diseases, metabolism and organismal systems. Among them, the pathways involved in DMs are mainly ferroptosis, ABC transporters, purine metabolism, carbon metabolism, biosynthesis of amino acids, and protein digestion and absorption. The pathways involved in DEPs are mainly endocytosis, protein processing in endoplasmic reticulum, oxidative phosphorylation and thermogenesis. Since iron metabolism may affect cellular processes, the top 10 cellular processes in the pathway, as shown in Fig. 4**c**, including tight junction, regulation of actin cytoskeleton, focal adhesion, autophagy - animal, cellular senescence, phagosome, ferroptosis, peroxisome and adherens junction were further screened in the study.

The metabolic pathways involved in DMs and DEPs were screened using metabolomics and proteomics approaches (Fig. 4 a and b), and a combined analysis of metabolomics and proteomics was performed using the KEGG pathway as a vector. Interworking Network and Venn diagram showed the status of KEGG pathway interactions involving metabolomics and proteomics (Fig. 4 d and e), with 58 metabolic pathways screened by metabolomics and proteomics identified 49 metabolic pathways, of which 15 metabolic pathways overlapped between the two. Fig. 4**e** shows the 15 metabolic pathways shared by metabolomics and proteomics, and notably, the iron metabolic pathway (ferroptosis) was found among the pathways.

3.5. Iron metabolic pathway analysis

To better understand the linkages between DMs, DEPs and metabolic pathways involved in iron metabolism, DMs and DEPs involved in iron metabolism (ferroptosis) were identified. As shown in Fig. 5 a and b, four DMs were identified, including L-glutamic acid, arachidonic acid, glutathione and gamma-glutamylcysteine. Five DEPs were found, including ferritin, phospholipid hydroperoxide glutathione peroxidase, heme oxygenase 1, major prion protein and acyl-CoA synthetase long chain family member 4. The pathway-pathway interaction network diagram drawn by four DMs and five DEPs (Fig. 5c) showed that the

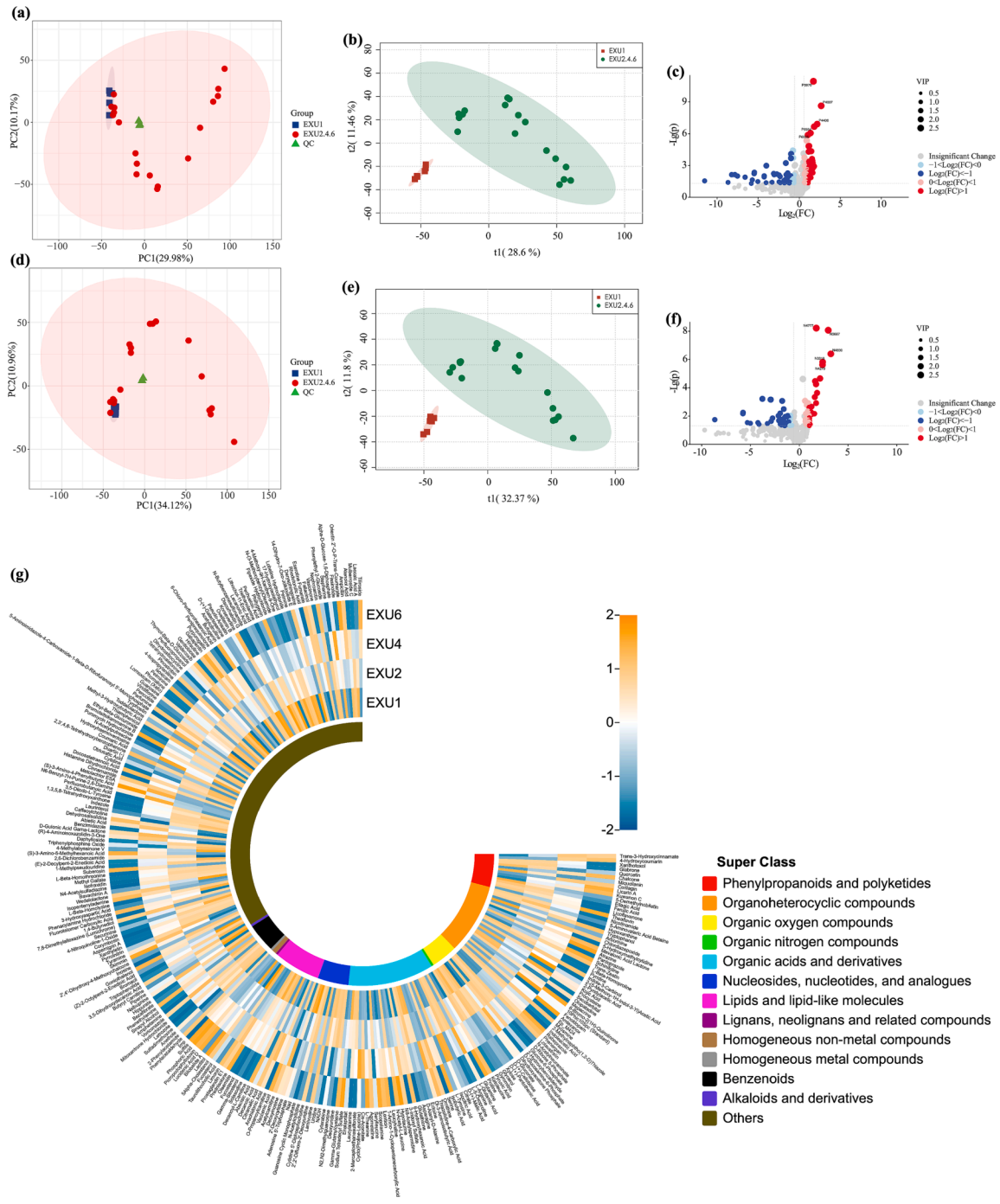

Fig. 2. Metabolite profiles based on metabolomics. (a) PCA analysis of metabolites in POS. (b) PLS-DA analysis of metabolites in POS. (c) Volcano map for screening DMs in POS. (d) PCA analysis of metabolites in NEG. (e) PLS-DA analysis of metabolites in NEG. (f) Volcano map for screening DMs in NEG. (g) Heat map of clustering of DMs.

process of iron metabolism (ferroptosis) was not isolated, and the process of iron metabolism was jointly regulated by the interaction between DMs and DEPs.

4. Discussion

Ageing is the most common treatment of meat in order to achieve satisfactory meat quality (della Malva, Gagaoua, Santillo, De Palo, Sevi & Albenzio, 2022). However, not all effects of the ageing process are positive, and longer ageing times lead to reduced oxidative stability, which in turn reduces the quality of the meat (Yu et al., 2023). After slaughter, muscle oxidation is inevitable and involves a series of metabolic pathways, including glycolysis, mitochondrial respiratory chain and nitric oxide accumulation (Chen et al., 2022; Liu, Hu, Zheng, Ma & Liu, 2022). Iron ions in muscle oxidation are usually overlooked. However, our previous study found that iron overload induced protein and lipid oxidation (Liu, Liu, Zheng & Ma, 2022). Currently, the analysis of meat quality and potential biochemical processes during ageing relies on muscle tissue (della Malva et al., 2022). Muscle tissue has similar metabolite types and levels to its exudates, which reflects the potential value of exudates for providing information about meat characteristics (Castejón, García-Segura, Escudero, Herrera & Cambero (2015). In this

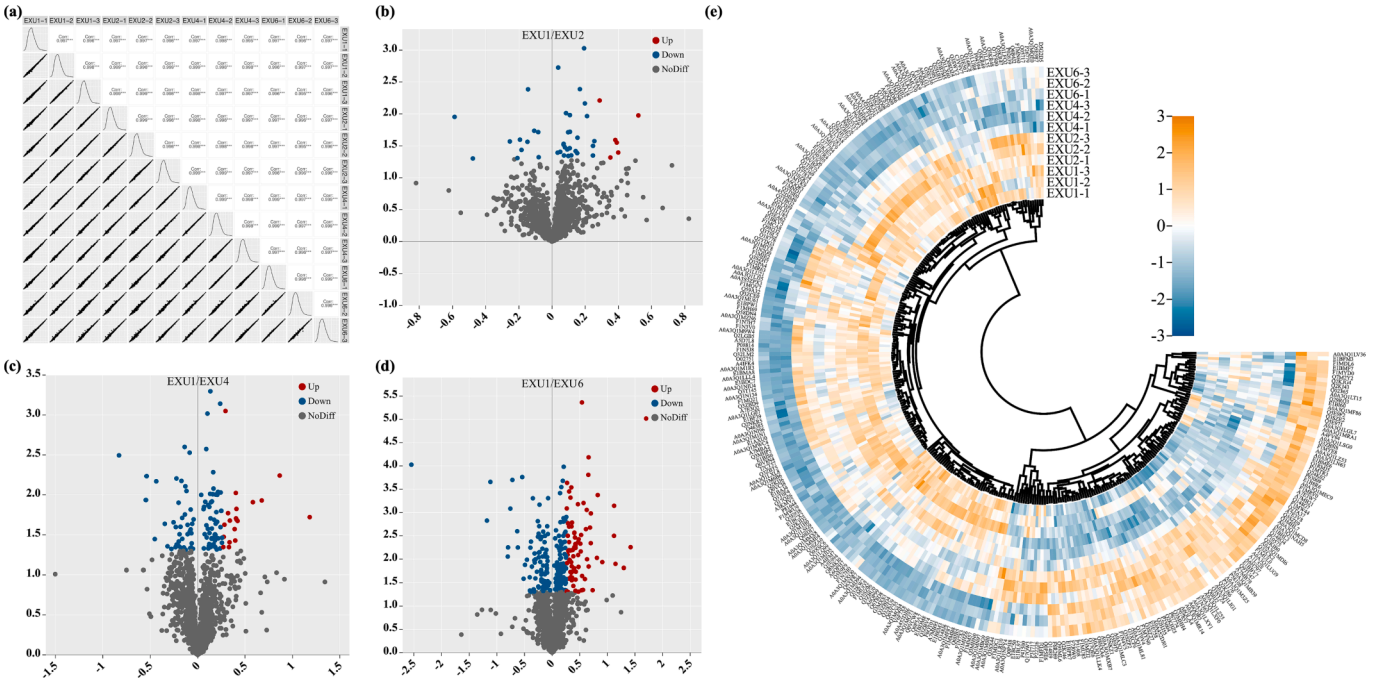

Fig. 3. Protein profiles based on proteomics. (a) Correlation coefficient plots of protein expression patterns of different groups. (b) Volcano map of DEPs between B1 and B2. (c) Volcano map of DEPs between B1 and B4. (d) Volcano plot of DEPs between B1 and B6. (e) Heat map of clustering of DEPs.

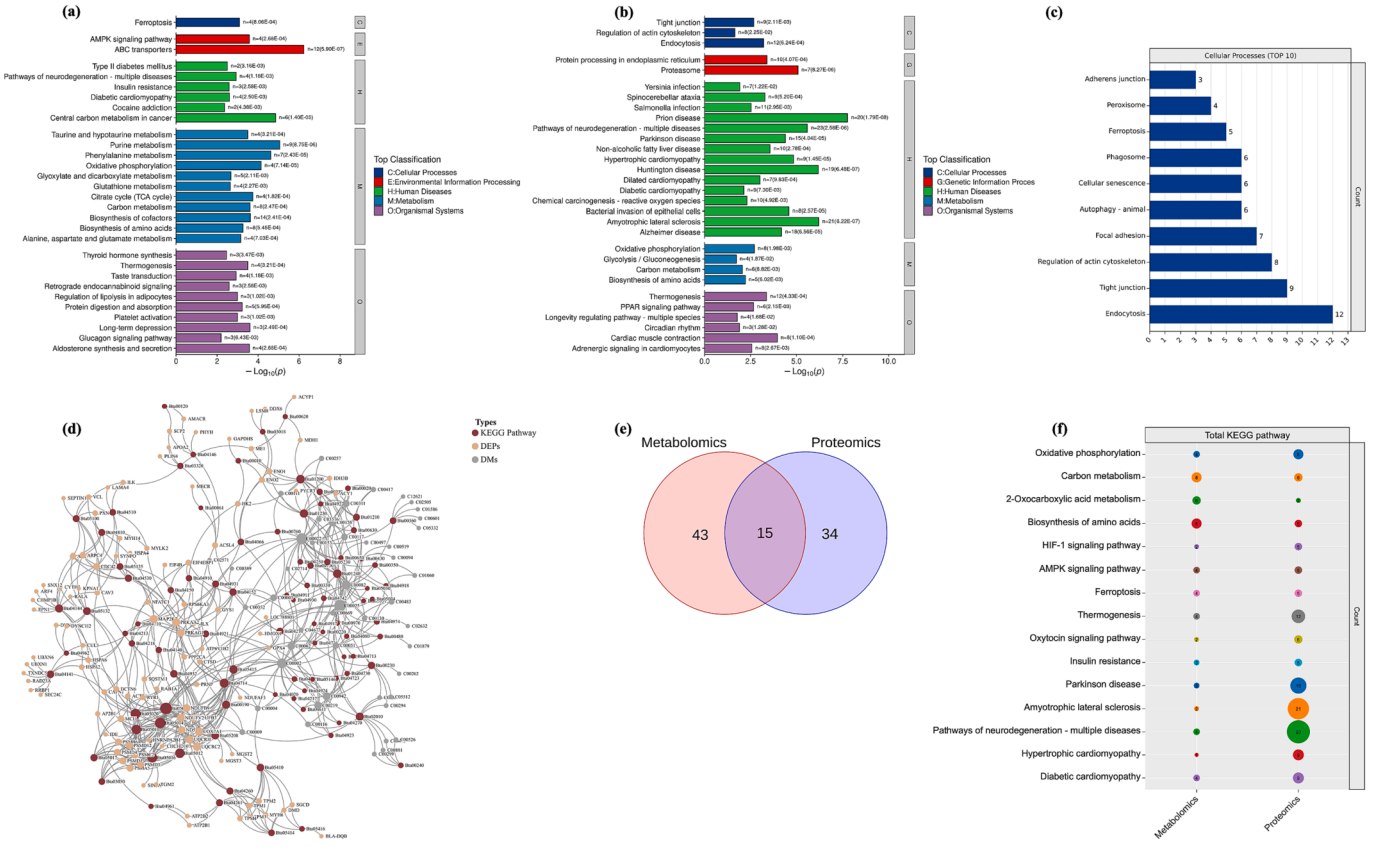

Fig. 4. Metabolic pathway analysis based on metabolomics and proteomics. (a) KEGG enrichment pathway analysis based on metabolomics. (b) KEGG enrichment pathway analysis based on proteomics. (c) Proteomics-based cellular process pathways for KEGG enrichment (top 10). (d) Network diagram of metabolomics and proteomics combined analysis. (e) Venn diagram of KEGG enrichment pathways based on metabolomics and proteomics. (f) Shared pathways of metabolomics and proteomics based on KEGG enrichment. C is Cellular Processes, E is Environmental Information Processing, H is Human Diseases, M is Metabolism, O is Organismal Systems.

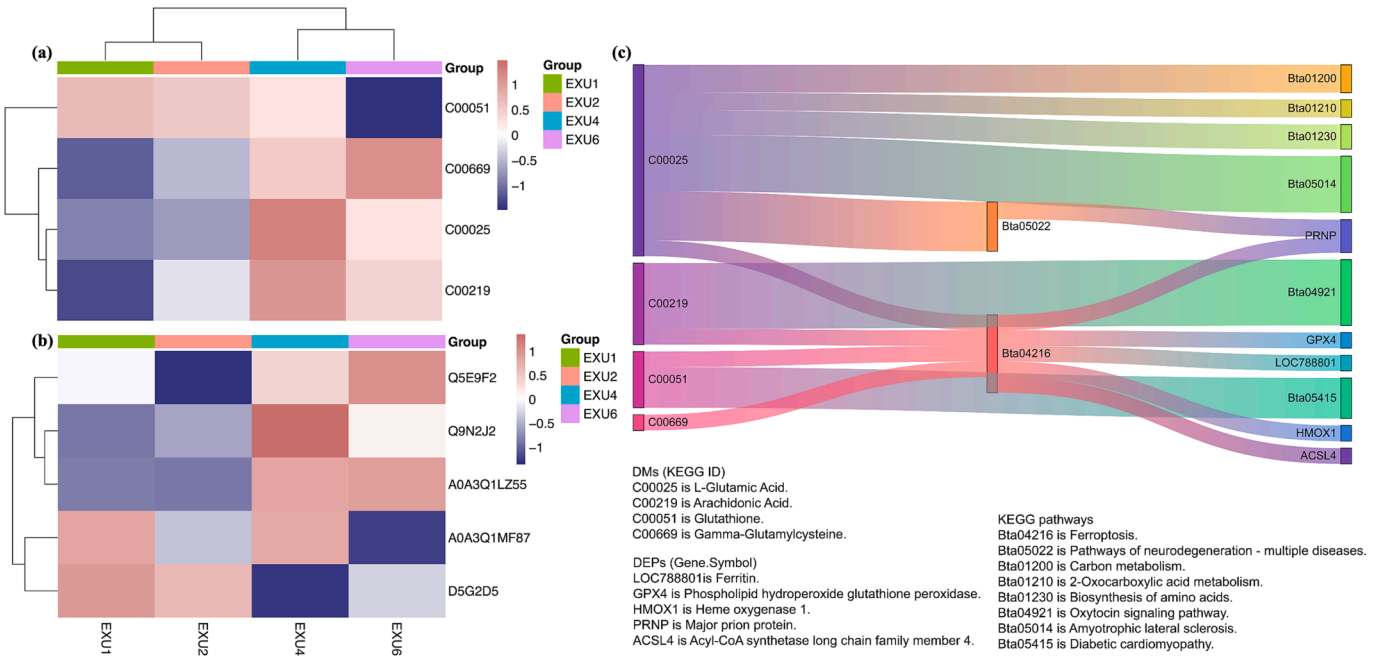

Fig. 5. Iron metabolism pathway. (a) Cluster heat map of DMs involved in iron metabolism. (b) Heat map of DEPs involved in iron metabolism. (c) Sankey diagram of the interaction network of DMs-DEPs-metabolic pathways based on ferroptosis pathways. A0A3Q1MF87 is ferritin, Q9N2J2 is phospholipid hydroperoxide glutathione peroxidase, Q5E9F2 is heme oxygenase 1, D5G2D5 is major prion protein, A0A3Q1LZ55 is acyl-CoA synthetase long chain family member 4.

research, 877 metabolites and 1957 proteins were identified in exudate, and the physicochemical characteristics of exudate, including iron content, protein and lipid oxidation status, were consistent with beef expression trends (Fig. 1), indicating that exudate can be used for characterizing the underlying biochemical processes of beef oxidation.

In the case of beef, a red meat is because bovine muscle is a β-red fiber and contains high amounts of iron, which is present in the muscle in the form of heme. Iron-containing hemoglobin is retained in muscle tissue in the form of blood residues. In addition, iron is present in macromolecular fractions, such as cytochromes, iron-sulfur proteins and iron carrier proteins (Liu et al., 2022). These iron-containing proteins provide carriers for the release of free iron or low-molecular-weight iron, the released iron ions generate hydroxyl radicals (•OH) through the Fenton reaction, and •OH is considered the most powerful oxidant known to oxidize lipids and proteins, leading to the deterioration of meat quality (Zhang et al., 2022). Ferroptosis has been found in muscle tissues, and the accumulation of free iron is central to the generation of ROS and mediates cell death. Thus, it is clarified that iron ions act as a destabilizing factor that reduces muscle quality through metabolic activity (Liu, Hu, Ma, Yang, Zheng & Liu, 2023). Notably, we previously used exudate to investigate the mechanisms of beef quality change, and found that abnormal iron metabolism activated the ferroptosis pathway, inducing oxidative stress in muscle tissue cells (Liu et al., 2022). Ferroptosis is a non-apoptotic regulation of cell death by iron-dependent lipid peroxidation due to unstable iron accumulation and glutathione peroxidase (GPX) 4 inactivation. At the core of this is the induction of lipid reactive oxygen species (ROS) accumulation by iron overload through the Fenton reaction (Xia et al., 2021a,b). Free iron levels in exudate and beef significantly increased during ageing (Fig. 1a, $P < 0.05$), leading to an increase in iron metabolic instability. At the same time, muscle ROS levels were accompanied by the accumulation of iron ions, leading to the oxidation of proteins and lipids (Fig. 1i). Overall, further studies in the expression patterns of metabolites and proteins in exudate are needed to reveal the mechanisms of iron metabolism in muscle oxidation during aging.

Homeostatic imbalances in iron metabolism affect normal physiological pathways, and iron overload is a critical factor in iron metabolism (Xie, Fang & Zhang, 2023). Bioinformatic analysis of exudate metabolites and proteins identified the only iron metabolic process, namely ferroptosis (Fig. 4**f**). As illustrated in **Fig. S1**, ferroptosis involves inactivation of GPX4 antioxidant action, lipid peroxidation, degradation of iron-containing proteins and conversion of iron ion valence states. As the name implies, iron accumulation is the key hub of ferroptosis, and the ferroptosis pathway shows the degradation of ferritin and heme to release free iron ions (**Fig. S1**). Ferritin is an iron storage protein that plays a central role in regulating iron metabolism and maintaining iron homeostasis. Ferritin is normally present in cells as ferritin light chain (FTL), heavy chain 1 (FTH1) and the constituent complexes, which can store more than 2000–4500 Fe^{3+} under normal physiological conditions. Consequently, ferritin can efficiently regulate intracellular iron homeostasis (Zhang, Yu, Song, Xiao, Xie & Xu, 2022). Notably, FTH1 and FTL exhibit different functional activities for iron binding. FTH1 has oxidase activity and converts soluble free iron in the cytoplasm into ferritin precursors that enter the ferritin structural domain and then bind to the inner ferritin space after conversion by the action of FTL (Zhang et al., 2022). Liu, Hu, Ma, Wang & Liu (2023) examined ferritin levels during beef refrigeration, and found that FTL and FTH1 exhibited different degradation states, which verified the different activity between FTH1 and FTL. The level of ferritin in the exudate tended to decrease during ageing (Fig. 5b), consistent with the findings of Liu et al. (2023). During ageing intracellular homeostasis is imbalanced and the selective autophagy receptor nuclear receptor coactivator (NCOA) 4 is activated to ensure cell survival, during which the inevitable NCOA4 binds to FTH1 and transports ferritin to the autophagosome for degradation (ferritinophagy), with eventual release of free iron (Xia et al., 2021b). **Fig. S1** shows the iron accumulation pathway of heme degradation by heme oxygenase (HO) 1. Heme is a ferroporphyrin compound composed of divalent iron with four porphyrin rings, primarily myoglobin and hemoglobin (Liu et al., 2022). The level of heme in muscle is related to the type of animal and the part of the meat. Lombardi-Boccia, Martinez-Dominguez, & Aguzzi (2002) examined the heme iron contents in different animals and different parts, and found that beef heme iron content was significantly higher than other meats. Thus, heme-rich beef has a higher potential for iron

ion release. Heme degradation relies mainly on the HO-1 catalytic system to release free iron (Singhabahu, Kodagoda Gamage & Gopalan, 2023). Free iron more readily mediates protein and lipid oxidation and is not heme (Zhang et al., 2022). Proteomics results showed a significant upregulation of HO-1 expression (Fig. 5b). Liu, Hu, Ma, Yang, Zheng & Liu (2023) analyzed the protein levels of HO-1 and heme, and found that the two were negatively correlated, consistent with the proteomics results. Overall, the degradation pathway of ferritin and heme during ageing is a key mechanism to induce iron sagging.

Iron ions can affect iron metabolism through transmembrane transport, with iron ions transferred intracellularly mainly via the transferrin (TF) and metal cation symporter ZIP8 (MCSZ8) pathways (**Fig. S1**). Proteomics identified a major prion protein (D5G2D5) that facilitates the conversion of trivalent to divalent iron ions (Fig. 5b), and its protein level decreased with increasing ageing duration. Iron ions are more sensitive to iron metabolic processes due to their higher oxidative activity as a result of valence conversion (Xia et al., 2021b). However, the reduced level of soft virus protein inhibited the cross-transport of iron ions by MCSZ8, while reducing the oxidative activity of divalent iron ions. On the other hand, the TF pathway is considered to be the main cell membrane ferric ion transport system (Wang, Wei, Ma, Qu & Liu, 2022), while there are different protein levels between TF and MCSZ8. Unfortunately, the effect of ferric ion transport across the membrane on cellular iron metabolism remains unknown.

Another hallmark event of iron metabolism disorders leading to ferroptosis is lipid oxidation, where polyunsaturated fatty acids (PUFAs) of cell or organelle membranes are susceptible to oxidation by ROS generated through the Fenton reaction and generate lipid peroxides (LPOs), the aggregation of which leads to membrane instability or even rupture, resulting in cellular homeostatic imbalance or even cell death (Liang, Zhang, Yang & Dong, 2019). Acyl-CoA synthetase long chain family (ACSL) 4 is a modulator of lipid metabolism. ACSL4 converts PUFAs to membrane phospholipids-phosphatidylethanolamine (PE) due to its thioesterified activity, forming PUFA-CoA. PUFA-CoA is a precursor of PUFA-phospholipids (PUFA-PLs), and PUFA-PLs are further oxidized by lipoxygenase to produce lipid peroxides (LOOHs, ·OH, etc.). Interestingly, arachidonic acid (AA) and epinephrine acyl contain a PE fraction, which facilitates lipid oxidation even more (Kagan et al., 2017; Yang, Kim, Gaschler, Patel, Shchepinov & Stockwell, 2016). The levels of both AA and ACSL4 increased during ageing (Fig. 5a and b), and the increase in AA content provides more substrate for ACSL4, which inevitably increases lipid peroxidation. There was a significant increase in lipid peroxidation (MDA level) in exudate and beef during late ageing (Fig. 1g, $P < 0.05$). It is noteworthy that ROS generated by the Fenton reaction are not specific for the oxidation of macromolecules and attack macromolecular components, such as proteins and DNA while oxidizing lipids, which inevitably enhances the oxidative state of the muscle (Liu et al., 2022). The increased carbonyl and sulfhydryl levels in exudate and beef indicate increased protein oxidation during ageing (Fig. 1 e and f, $P < 0.05$). Lipid and protein oxidation are not independent processes, but rather promote each other. For example, lipid peroxides bind to muscle proteins, and LOOHs and ·OH promote protein oxidation more rapidly (Liu et al., 2022).

The level of ROS generated by disorders of iron metabolism depends on sophisticated homeostatic regulatory functions of cells, and the classical mechanism of scavenging is through the glutathione peroxidase (GPX) 4 antioxidant system (Wang et al., 2022). GPX4 belongs to the glutathione peroxidase family, which specifically scavenges a wide range of lipid peroxides from cell membranes, and GPX4 is dependent on glutathione (GSH) as a reducing agent in its peroxidase action. GSH is a tripeptide synthesized from cysteine, glutamate and glycine. Cystine-glutamate antiporter pumps glutamate out of the cell and pumps cystine into the cell in a 1:1 ratio. The cystine delivered to the cell is reduced to cysteine by β-mercaptoethanol, which is used to synthesize the antioxidant GSH (Bi et al., 2023; Wang et al., 2022; Yang et al., 2016). GPX4 and GSH levels decreased during ageing (Fig. 5 a and b), indicating GPX4 may have a diminished effect on lipid peroxide scavenging, which can lead to an enhanced cellular or muscle oxidative state. In contrast, L-glutamic acid and gamma-glutamylcysteine levels were upregulated during aging, where higher levels of L-glutamic acid inhibited cystine transport, leading to a decrease in the content of GSH precursors (Liu et al., 2023). Carbon metabolism, 2-oxocarboxylic acid metabolism and biosynthesis of amino acids were also found to affect L-glutamic acid levels through glutamate-enriched metabolic pathways (Fig. 5c). For example, the 2-oxoglutarate dehydrogenase complex during carbon metabolism converts glutamate by catalyzing the conversion of 2-oxoglutarate generated in the tricarboxylic acid cycle (TCA) pathway, which may also lead to elevated glutamate levels (Weidinger et al., 2023). It is speculated that elevated gamma-glutamylcysteine levels may be associated with reduced glutathione synthetase activity, which requires further validation. The regulation of GSH-GPX4, an important intracellular antioxidantdoes not proceed independently, interacting with metabolic pathways, such as carbohydrates and amino acids, was not effective in avoiding oxidative stress induced by iron metabolism, reducing the quality of meat during aging. In general, the ferroptosis process is dependent on the accumulation of free iron, inactivation of antioxidant systems, and cell membrane lipid oxidation. These processes not only promote cell death, but also lead to deterioration of muscle quality through accumulation of ROS and lipid peroxides.

5. Conclusions

Exudate and beef were found to have similar patterns of change in terms of iron ions and oxidation. A combination of proteomics and metabolomics was used to identify the metabolite and protein changes that can be used to characterize the underlying biochemical pathways in muscle tissue. Overall, beef exudates provide valuable information to understand metabolic mechanisms during muscle aging. A total of 15 shared KEGG pathways were identified, and iron metabolism was mainly manifested as ferroptosis. The 4 DMs and 5 DEPs involved in the ferroptosis pathway may induce oxidative stress and even cell death through the regulation of free iron accumulation, cell or organelle membrane oxidation and GPX4, exacerbating muscle protein and lipid oxidation during aging.

Funding

This study was financially supported by the Ningxia Natural Science Foundation (2022AAC02021), Hubei Normal University 2023 introduced talent research start-up fund, and Excellent Young and Middle-Aged Science and Technology Innovation Team Plan Project of University in Hubei Province (T2022028), and Hubei Provincial Natural Science Foundation-Joint Fund Program (2023AFD025).

CRediT authorship contribution statement

Jun Liu: Writing – review & editing, Writing – original draft, Visualization, Validation, Resources, Investigation, Formal analysis, Data curation, Conceptualization. **Cuili Pan:** Supervision, Funding acquisition. **Hui Yue:** Formal analysis. **He Li:** Formal analysis. **Dunhua Liu:** Visualization, Supervision, Project administration, Funding acquisition, Conceptualization. **Ziying Hu:** Formal analysis, Investigation. **Yuanliang Hu:** Investigation. **Xiang Yu:** Investigation. **Weiwei Dong:** Investigation. **Yanli Feng:** Investigation.

Declaration of competing interest

The authors declare that they have no known competing financial interests or personal relationships that could have appeared to influence the work reported in this paper.

Data availability

Data will be made available on request.

Acknowledgments

Thanks to Gaolong Yin at Shanghai Bioprofile Technology Company Ltd. for his technical support in proteomics. Thanks to Prof. Deming Gong of the New Zealand Institute of Natural Medicine Research for proofreading the language of the article.

Appendix A. Supplementary data

Supplementary data to this article can be found online at https://doi.org/10.1016/j.fochx.2023.101038.

References

Bi, Y., Liu, S., Qin, X., Abudureyimu, M., Wang, L., Zou, R., … Zhang, Y. (2023). FUNDC1 interacts with GPx4 to govern hepatic ferroptosis and fibrotic injury through a mitophagy-dependent manner. *Journal of Advanced Research*. https://doi.org/10.1016/j.jare.2023.02.012

Castejón, D., García-Segura, J. M., Escudero, R., Herrera, A., & Cambero, M. I. (2015). Metabolomics of meat exudate: Its potential to evaluate beef meat conservation and aging. *Analytica Chimica Acta, 901*, 1–11. https://doi.org/10.1016/j.aca.2015.08.032

Chen, C., Guo, Z., Shi, X., Guo, Y., Ma, G., Ma, J., & Yu, Q. (2022). H_2O_2-induced oxidative stress improves meat tenderness by accelerating glycolysis via hypoxia-inducible factor-1α signaling pathway in postmortem bovine muscle. *Food Chemistry: X, 16*, Article 100466. https://doi.org/10.1016/j.fochx.2022.100466

Chen, C., Zhang, J., Guo, Z., Shi, X., Zhang, Y., Zhang, L., … Han, L. (2020). Effect of oxidative stress on AIF-mediated apoptosis and bovine muscle tenderness during postmortem aging. *Journal of Food Science, 85*(1), 77–85. https://doi.org/10.1111/1750-3841.14969

Della Malva, A., Gagaoua, M., Santillo, A., De Palo, P., Sevi, A., & Albenzio, M. (2022). First insights about the underlying mechanisms of Martina Franca donkey meat tenderization during aging: A proteomic approach. *Meat Science, 193*, Article 108925. https://doi.org/10.1016/j.meatsci.2022.108925

Hu, Z., Ma, Y., Liu, J., Fan, Y., Zheng, A., Gao, P., … Liu, D. (2022). Assessment of the Bioaccessibility of Carotenoids in Goji Berry (Lycium barbarum L.) in Three Forms: In Vitro Digestion Model and Metabolomics Approach. *Foods, 11*(22), 3731. https://doi.org/10.3390/foods11223731

Huang, Y., Xie, Y., Li, Y., Zhao, M., Sun, N., Qi, H., & Dong, X. (2023). Quality assessment of variable collagen tissues of sea cucumber (Stichopus japonicus) body wall under different heat treatment durations by label-Free proteomics analysis. *Food Research International, 165*, Article 112540. https://doi.org/10.1016/j.foodres.2023.112540

Kagan, V. E., Mao, G., Qu, F., Angeli, J. P. F., Doll, S., Croix, C. S., … Bayır, H. (2017). Oxidized arachidonic and adrenic PEs navigate cells to ferroptosis. *Nature Chemical Biology, 13*(1), 81–90. https://doi.org/10.1038/NCHEMBIO.2238

Kim, Y. H. B., Ma, D., Setyabrata, D., Farouk, M. M., Lonergan, S. M., Huff-Lonergan, E., & Hunt, M. C. (2018). Understanding postmortem biochemical processes and post-harvest ageing factors to develop novel smart-ageing strategies. *Meat Science, 144*, 74–90. https://doi.org/10.1016/j.meatsci.2018.04.031

Lepper-Blilie, A. N., Berg, E. P., Buchanan, D. S., & Berg, P. T. (2016). Effects of post-mortem ageing time and type of ageing on palatability of low marbled beef loins. *Meat Science, 112*, 63–68. https://doi.org/10.1016/j.meatsci.2015.10.017

Liang, C., Zhang, X., Yang, M., & Dong, X. (2019). Recent Progress in Ferroptosis Inducers for Cancer Therapy. *Advanced Materials, 31*(51), 1904197. https://doi.org/10.1002/adma.201904197

Liu, J., Hu, Z., Liu, D., Zheng, A., & Ma, Q. (2023). Glutathione metabolism-mediated ferroptosis reduces water-holding capacity in beef during cold storage. *Food Chemistry, 398*, Article 133903. https://doi.org/10.1016/j.foodchem.2022.133903

Liu, J., Hu, Z., Ma, Q., Wang, S., & Liu, D. (2023). Ferritin-dependent cellular autophagy pathway promotes ferroptosis in beef during cold storage. *Food Chemistry, 412*, Article 135550. https://doi.org/10.1016/j.foodchem.2023.135550

Liu, J., Hu, Z., Ma, Q., Yang, C., Zheng, A., & Liu, D. (2023). Reduced water-holding capacity of beef during refrigeration is associated within creased heme oxygenase 1 expression, oxidative stress and ferroptosis. *Meat Science, 202*, Article 109202. https://doi.org/10.1016/j.meatsci.2023.109202

Liu, J., Hu, Z., Zheng, A., Ma, Q., & Liu, D. (2022). Identification of exudate metabolites associated with quality in beef during refrigeration. *LWT - Food Science and Technology, 172*, Article 114241. https://doi.org/10.1016/j.lwt.2022.114241

Liu, J., Liu, D., Wu, X., Pan, C., Wang, S., & Ma, L. (2022). TMT quantitative proteomics analysis reveals the effects of transport stress on iron metabolism in the liver of chicken. *Animals, 12*(1), 52. https://doi.org/10.3390/ani12010052

Liu, J., Liu, D., Zheng, A., & Ma, Q. (2022). Haem-mediated protein oxidation affects water-holding capacity of beef during refrigerated storage. *Food Chemistry: X, 100304*. https://doi.org/10.1016/j.fochx.2022.100304

Lombardi-Boccia, G., Martinez-Dominguez, B., & Aguzzi, A. (2002). Total heme and non-heme iron in raw and cooked meats. *Journal Of Food Science, 67*(5), 1738–1741. https://doi.org/10.1111/j.1365-2621.2002.tb08715.x

Marcondes Krauskopf, M., Darlan Leal de Araújo, C., dos Santos-Donado, P. R., Damiames Baccarin Dargelio, M., Antônio Santos Manzi, J., Cecilia Venturini, A., César de Carvalho Balieiro, J., Francisquine Delgado, E., & Contreras-Castillo, C. J. (2023). The effect of succinate on color stability of Bos Indicus bull meat: pH-dependent effects during the 14-day aging period. Food Research International, 113688. doi: 10.1016/j.foodres.2023.113688.

Setyabrata, D., Ma, D., Xie, S., Thimmapuram, J., Cooper, B. R., Aryal, U. K., & Kim, Y. H. B. (2023). Proteomics and metabolomics profiling of meat exudate to determine the impact of postmortem ageing on oxidative stability of beef muscles. *Food Chemistry: X, 18*, Article 100660. https://doi.org/10.1016/j.fochx.2023.100660

Singhabahu, R., Kodagoda Gamage, S. M., & Gopalan, V. (2023). Pathological significance of heme oxygenase-1 as a potential tumor promoter in heme-induced colorectal carcinogenesis. *Cancer Pathogenesis and Therapy*. https://doi.org/10.1016/j.cpt.2023.04.001

Wang, S., Wei, W., Ma, N., Qu, Y., & Liu, Q. (2022). Molecular mechanisms of ferroptosis and its role in prostate cancer therapy. *Critical Reviews in Oncology/Hematology, 176*, Article 103732. https://doi.org/10.1016/j.critrevonc.2022.103732

Wang, Y., Li, W., Zhang, C., Li, F., Yang, H., & Wang, Z. (2023). Metabolomic comparison of meat quality and metabolites of geese breast muscle at different ages. *Food Chemistry: X, 19*, Article 100775. https://doi.org/10.1016/j.fochx.2023.100775

Wang, Z., Li, X., Lu, K., Wang, L., Ma, X., Song, K., & Zhang, C. (2023). Effects of dietary iron levels on growth performance, iron metabolism and antioxidant status in spotted seabass (Lateolabrax maculatus) reared at two temperatures. *Aquaculture, 562*, Article 738717. https://doi.org/10.1016/j.aquaculture.2022.738717

Weidinger, A., Milivojev, N., Hosmann, A., Duvigneau, J. C., Szabo, C., Törö, G., … Kozlov, A. V. (2023). Oxoglutarate dehydrogenase complex controls glutamate-mediated neuronal death. *Redox Biology, 62*, Article 102669. https://doi.org/10.1016/j.redox.2023.102669

Xia, J., Si, H., Yao, W., Li, C., Yang, G., Tian, Y., & Hao, C. (2021a). Research progress on the mechanism of ferroptosis and its clinical application. *Experimental Cell Research, 409*(2), Article 112932. https://doi.org/10.1016/j.yexcr.2021.112932

Xia, X., Cheng, Z., He, B., Liu, H., Liu, M., Hu, J., … Bai, Y. (2021bf). Ferroptosis in aquaculture research. *Aquaculture, 541*, Article 736760. https://doi.org/10.1016/j.aquaculture.2021.736760

Xie, L., Fang, B., & Zhang, C. (2023). The role of ferroptosis in metabolic diseases. Biochimica et Biophysica Acta (BBA) - Molecular. *Cell Research, 1870*(6), Article 119480. https://doi.org/10.1016/j.bbamcr.2023.119480

Yang, W. S., Kim, K. J., Gaschler, M. M., Patel, M., Shchepinov, M. S., & Stockwell, B. R. (2016). Peroxidation of polyunsaturated fatty acids by lipoxygenases drives ferroptosis. *Proceedings of the National Academy of Sciences, 113*(34), E4966–E4975. https://doi.org/10.1073/pnas.1603244113

Yu, Q., Cooper, B., Sobreira, T., & Kim, Y. H. B. (2021). Utilizing Pork Exudate Metabolomics to Reveal the Impact of Ageing on Meat Quality. *Foods, 10*(3), 668. https://doi.org/10.3390/foods10030668

Yu, Q., Li, S., Cheng, B., Brad Kim, Y. H., & Sun, C. (2023). Investigation of changes in proteomes of beef exudate and meat quality attributes during wet-aging. *Food Chemistry: X, 17*, Article 100608. https://doi.org/10.1016/j.fochx.2023.100608

Zhang, J., Yu, Q., Han, L., Han, M., & Han, G. (2020). Effects of lysosomal iron involvement in the mechanism of mitochondrial apoptosis on postmortem muscle protein degradation. *Food Chemistry, 328*, Article 127174. https://doi.org/10.1016/j.foodchem.2020.127174

Zhang, N., Yu, X., Song, L., Xiao, Z., Xie, J., & Xu, H. (2022). Ferritin confers protection against iron-mediated neurotoxicity and ferroptosis through iron chelating mechanisms in MPP+-induced MES23.5 dopaminergic cells. *Free Radical Biology and Medicine, 193*, 751–763. https://doi.org/10.1016/j.freeradbiomed.2022.11.018

Zhang, Y., Tian, X., Jiao, Y., Wang, Y., Dong, J., Yang, N., … Wang, W. (2022). Free iron rather than heme iron mainly induces oxidation of lipids and proteins in meat cooking. *Food Chemistry, 382*, Article 132345. https://doi.org/10.1016/j.foodchem.2022.132345